Revised: 21 March 2021 | Accepted: 29 March 2021

DOI: 10.1002/ces2.10087

ORIGINAL ARTICLE

International Journal of Ceramic Engineering & Science

Colloidal processing and characterization of TiO_2–MnO-doped alumina/alumina slurries and tapes

Marcelo Daniel Barros[1,2] | **Dachamir Hotza**[1] | **Rolf Janssen**[2]

[1]Graduate Program in Materials Science and Engineering (PGMAT), Laboratory of Ceramics Processing (PROCER), Federal University of Santa Catarina (UFSC), Florianópolis, Brazil

[2]Institute of Advanced Ceramics, Hamburg University of Technology (TUHH), Hamburg, Germany

Correspondence
Rolf Janssen, Institute of Advanced Ceramics, Hamburg University of Technology (TUHH), Hamburg 21073, Germany.
Email: janssen@tuhh.de

Funding information
Deutscher Akademischer Austauschdienst; CAPES; German Research Foundation (DFG), Grant/Award Number: 192, 346071 and SFB 986; CAPES/PRINT, Grant/Award Number: 88881.310728/2018-0

Abstract

Aqueous slurries of alumina doped with manganese and titanium oxides were developed. The powders and tapes were investigated by scanning electron (SEM) microscopy, X-ray diffractometry (XRD), and thermal analyses (TG/DSC). The stability and rheology of colloidal suspensions of undoped and doped alumina suspensions were investigated. At neutral pH of 7, pure alumina and MnO–TiO_2 dopant particles present positive and negative surface charges and are prone to heterocoagulation. Optimized colloidal processing through proper adjustment of parameters was achieved to reach particle stabilization. The surface charge of the oxide particles was negative, and the suspensions did not agglomerate at a pH of 7 and higher. Tapes were cast, dried, and burned out. The thermal analyses revealed the release of residual water and decomposition of short-chain organics at temperatures under 215°C and of long-chain additives over 300°C.

KEYWORDS

alumina, colloidal processing, manganese oxide, tape casting, titanium dioxide

1 | INTRODUCTION

Tape casting is a wet-shaping process for producing flat and thin ceramics sheets with thicknesses in the range of 1-1000 μm.[1,2] This technique is applied to produce electronic substrates, multilayered capacitors, piezoceramics, solid oxide fuel cells' components, functionally graded materials, and porous membranes or substrates. Tape casting slurries are typically composed of ceramic powder, solvent (water or organic), and additives such as dispersants, binders, plasticizers, and antifoams.[3,4] These components are put together in the milling and mixing steps, in the correct order to ensure the slurry homogeneity and a typical pseudoplastic rheological behavior.[5] The processing of tapes consists of casting a ceramic slurry through a leveling blade with a preset gap over a collector film, forming the continuous tape.[6] Several non-oxide and oxide ceramic tapes, particularly alumina, have been developed and produced.[7–13]

The slurry optimization is a critical step in this processing, that is, defining the amount of each component, choosing additives, and consolidating the preparation procedure. Taking into account environmental and safety issues, the importance of using water as a solvent to produce tapes is increasing. Some advantages of the aqueous route are non-inflammability, non-toxicity, and relatively low cost.[14–17] However, the search for a suitable water-based slurry faces some challenges regarding the rheological and drying behaviors.[8] The surface charge of powders is an important property for processing colloidal routes, which is characterized by the zeta potential.[18] Thereby, the isoelectric point (IEP) corresponds to a pH value or range denoting a tendency for agglomeration when the zeta potential approaches zero.[19]

When different oxides are mixed in a suspension, even in low amounts, a so-called heterocoagulation occurs when, at a certain pH, the particle surfaces are positively and negatively charged, and attract each other.

An aqueous slurry is a complex multiphase system with low tolerance to changes in drying conditions, casting composition, and film thickness. Crack-free uniform green tapes are possible only when all variables are well controlled.[20,21] Good quality tapes are characterized by the absence of defects during drying, handling, homogeneity and lamination, debinding, and sintering high capabilities. The subsequent removal of organics is normally carried out via burnout at low temperatures (<500°C) using a very low heating rate. Thereby, the heating up needs to be designed in a way that the components' evaporation rate does not surpass the diffusion rate. Otherwise, the vapor formed inside the green material can lead to the formation of cracks and defects.[5,14]

In a former work, doped and undoped alumina tapes were used to produce ceramic laminates with alternating layers of high and low sinterability.[22] Nevertheless, the slurry stability and rheology were not characterized or optimized. The challenge is to obtain a more homogeneous distribution of dopants within the alumina matrix during sintering, which will be further discussed with the focus on the diffusion of the dopants in sintered laminates.[23]

In the present work, MnO and TiO_2 are added to Al_2O_3 as sintering aids. Since the diffusion of nanocomponents is intrinsically related to homogeneously distributed dopants in the matrix, the key point is to guarantee that the particles of titanium and manganese oxide are well dispersed right from the beginning within the aqueous suspension. An optimization of colloidal processing features to avoid particle agglomeration is mandatory. Therefore, the focus of this work is to produce defect-free ceramic tapes to be submitted to thermal treatments.

2 | MATERIALS AND METHODS

2.1 | Oxide powders

To produce ceramic tapes, two types of alumina and two sintering aids were used as starting powders (Table 1). The matrix powders were high purity 0.10 μm alumina powder (Taimicron TM-DAR, Taimei Chemicals), named F for finer, and 0.40 μm alumina (CT 3000 SG, Almatis), named C for coarser. Fine alumina (F) doped with titanium dioxide and manganese oxide was produced using high-energy ball milling (PE075, Netzsch), and named D for doped. In this case, the Taimicron TM-DAR was used as the main powder, together with 1.68 wt% of titanium dioxide (RD3, Kemira Oyj) and 2.32 wt% of manganese oxide (manganese (II) oxide; Sigma-Aldrich). A 500 cm^3 alumina crucible, 1400 *g* of 3 mm diameter zirconia balls (YTZ®, Nikkato), and 200 mL of ethanol 99% were used as grinding and liquid media, respectively. Attrition milling was performed on 160 g powder batches at 600 RPM for 2 h. After milling, the mixture was dried in air at room temperature and sieved with a 200 μm open sieve in a vibratory sieve shaker (AS 200 Digit cA; Retsch).

To characterize the raw powders, scanning electron microscopy (TM 3030; Hitachi) was performed with 15 kV. Particle size distribution (PSD) was measured by dynamic light scattering (DLS, Zetasizer Nano ZS, Malvern Panalytical) in aqueous suspensions with 0.01 wt% of powder. Zeta potential (ZP) was measured (Zetasizer Nano ZS, Malvern Panalytical) with automatic titration using NaOH and HCl solutions for pH from 2 to 12. In both PSD and ZP analyses, 1 wt% (referred to solids) of ammonium polymethacrylate solution (Darvan C-N; Vanderbilt) was used as a dispersant, and samples were ball milled for 4 h. X-ray diffraction was performed at room temperature in a diffractometer (Miniflex; Rigaku) in the 2θ angle range varying from 5º to 90º, and crystalline phases were characterized using a database (PDF-2, ICDD). The doped alumina powder quantification of crystalline phases was measured using the Rietveld refinement method with a powder pattern analysis software (X'Pert HighScore Plus, Malvern Panalytical).

2.2 | Processing of slurries and tapes

Optimization of solids content and preparation of slurries were previously set:[24] 21 vol% of solids for undoped and doped fine alumina (F and D), 25 vol% of solids for coarse, pure alumina (C). For calculating the powder quantities, the density of 3.96 g/cm^3 for F and C, and 4.00 g/cm^3 for D were used. In the first step, the powder was deagglomerated in deionized water with the addition of 2 wt%, referred to solids content, of the dispersing agent (Darvan C-N) using ball milling for 4 h. Then, a binder (Mowilith LDM 6138.BR Liq, Archroma), a non-ionic

TABLE 1 Oxide powders used for the production of ceramic tapes by tape casting

Name	Composition	Brand name	d_{50} (μm)	ρ (g/cm^3)	Function
F	α-Al_2O_3	Taimei Chemicals	0.10	3.96	Matrix
C	α-Al_2O_3	Almatis	0.40	3.90	Matrix
M	MnO	Sigma-Aldrich	8.00	5.45	Dopant
T	TiO_2 (rutile)	Kemira	0.08	4.00	Dopant

surfactant (Ninol PK-80 BR, Stepan), and an antifoamer (Antifoam Y-30, Sigma-Aldrich) were added with 30, 1.5, and 1 wt%, respectively, referred to solids, and ball milled for more 30 min. Slurries were placed in an ultrasonic bath (Q1.8L, Eco-Sonics) for 5 min and left to rest for 1 h to ensure all bubble removal.

The rheological behavior of slurries was analyzed with a shear-controlled rotation viscometer (550 Haake™ Viscotester™, Thermo Fischer) with concentric cylinders (SV2P), coupled with a temperature controller (DC-10, Thermo Fischer). Tests were performed at 25°C, at shear rates varying from 0.02 to 500 s^{-1}. Between the ramps of increasing and decreasing shear rate, a plateau of 60 s was set at 500 s^{-1}. Fitting was carried out according to Herschel-Bulkley model using dedicated software (Haake™ RheoWin™, Thermo Fischer).

The slurries were cast on a silicone-coated Mylar® band at a casting speed of 6 cm/min using a tape casting machine (CC-1200, Tape Casting Warehouse). Tapes were then dried in air at room temperature for 24 h. The upper and bottom surfaces of tapes were characterized using scanning electron microscopy (TM 3030, Hitachi) at a voltage of 15 kV on metalized surfaces. Differential scanning calorimetry analyses were performed together with thermogravimetry in a simultaneous thermal analyzer (TGA/DSC 1, Mettler-Toledo). As a reference, the fine alumina tape was used, since the organics constituents are the same for all tapes. The test was carried out in synthetic air (20% oxygen +80% nitrogen) from room temperature up to 550°C, at a heating rate of 1°C/min. After a dwell of 1 h, the sample was heated to 800°C with a heating rate of 5°C/min.

3 | RESULTS AND DISCUSSION

3.1 | Powders structure and composition

Figure 1 shows the micrographs of oxide powders used to produce the tapes. Alumina fine and coarse powders (F and C, respectively) presented faceted irregular shapes, while doped alumina powder (D) showed larger particles due to the mixing and drying processes which caused agglomeration.

Figure 2 presents the particle size distribution for the raw powders and Table 2 summarizes the values of d_{10}, d_{50}, and d_{90}. Particle size analyses showed that particle size distributions are unimodal for all powder. However, only the average particle size value provided by the manufacturer for the coarse alumina is comparable to the ones obtained by analyses. The d_{50} value of finer alumina is higher than that specified by the manufacturer, and the reason can be addressed to the formation of small agglomerates due to the high surface area of this powder, even using a dispersant. The undoped (F) and doped (D) fine alumina powder presented an almost similar value of d_{50}, corroborating the previous measurements and indicating the well-succeeded milling/mixing of added dopants, MnO and TiO_2, with no significant changes in the final particle size caused by the dopant addition.

Figure 3 shows the X-ray diffraction patterns of oxide powders, for 2θ ranging from 20º to 80º. The Al_2O_3 samples presented α-alumina phase (PDF 01-071-1683), while titanium dioxide and manganese oxide corresponded to rutile (PDF 01-078-1508) and cubic MnO (PDF 01-078-0424), respectively. The doped alumina system presented the three previously mentioned crystalline phases, and the Rietveld refinement quantified 95.8% for α-alumina, 1.9% for rutile, and 2.3% for cubic MnO.

3.2 | Slurries stabilization and rheology

Figure 4 presents the zeta potential variation as the function of pH for each powder, in suspensions with and without 1 wt% (referred to solids) of dispersant. Samples without dispersant presented isoelectric point 6.8 for F and 5.6 for D, indicating that the addition of MnO and TiO_2 as dopants slightly reduces the IEP of fine alumina suspension (F).

The isoelectric point for the coarse alumina (C) decreased from 7.9 to 4.3 when the dispersant was added. However, the

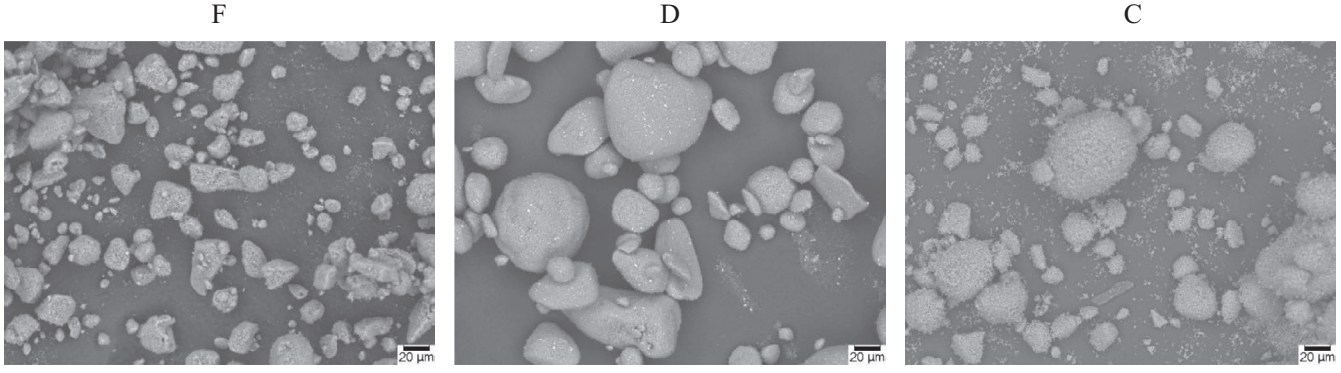

FIGURE 1 SEM micrographs of raw oxide powders used to produce the ceramic tapes. Samples F and C are finer and coarser alumina, respectively, as received. Sample D is fine doped alumina powder after milling and sieving

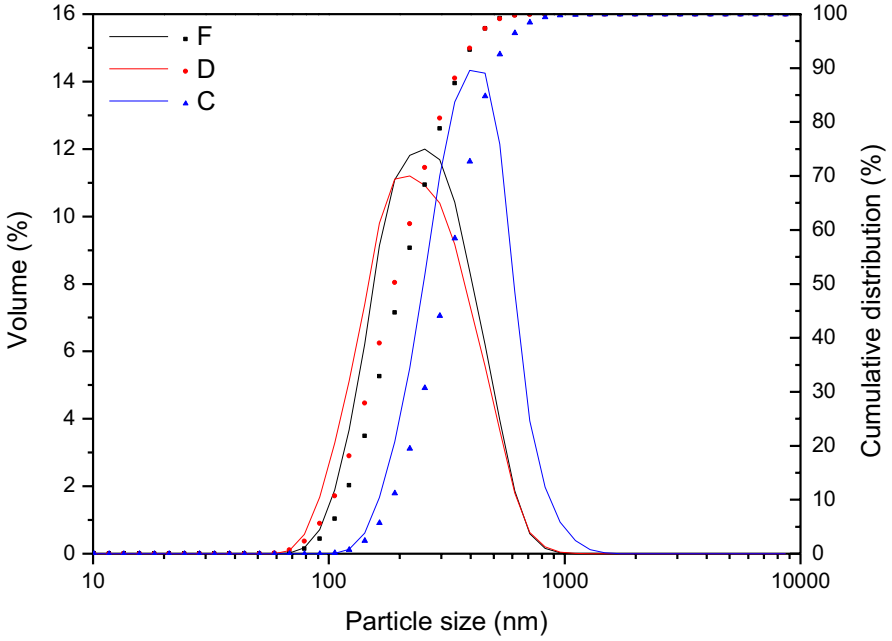

FIGURE 2 Particle size distribution of oxide powders. Volume, in percent, is plotted as non-cumulative and cumulative on the left and right *Y*-axis, respectively. C, coarse alumina; D, doped fine alumina; F, fine alumina

TABLE 2 Values of d_{10}, d_{50}, and d_{90} analyzed by DLS for the oxide powders

Powder samples	Average particle size (nm)		
	d_{10}	d_{50}	d_{90}
F	158	278	494
D	121	264	493
C	202	439	753

fine alumina samples (F, fine undoped, and D, fine doped) presented an IEP in the range of pH 2 after dispersant addition. The addition of MnO and TiO_2 as dopants produced no significant difference in the zeta potential curve of the fine alumina suspension (F) containing the dispersant. Therefore, the dispersant ensured the stability of the slurries since its addition shifted the alumina IEP to the pH range of 2-4.3. As reported in the literature, the IEP of pure alumina ranges from 8 to 9.3, and that of manganese and titanium oxide, from 5.4 to 5.9, depending on particle synthesis and purity.[25] Thus, in the present case, the IEP of Al_2O_3 was moved to the acidic range, such as those of MnO and TiO_2. The reason for this is linked to the good adsorption of dispersant (ammonium polymethacrylate) on ceramic particles, modifying the double electric layer and ensuring their repulsion. In this way, at neutral and basic pH values (7 and over), all oxides are negatively charged at the surface with zeta potential values lower than −40 mV, so that the particles remain dispersed.[18,26] The final tape casting slurries have been adjusted to pH values of 9.1, 9.1, and 8.9, for F, D, and C slurries, respectively. Thus, all of them were in the range of stability.

Figure 5 presents the rheological behavior of the ceramic slurries fitted by the Herschel-Bulkley model.

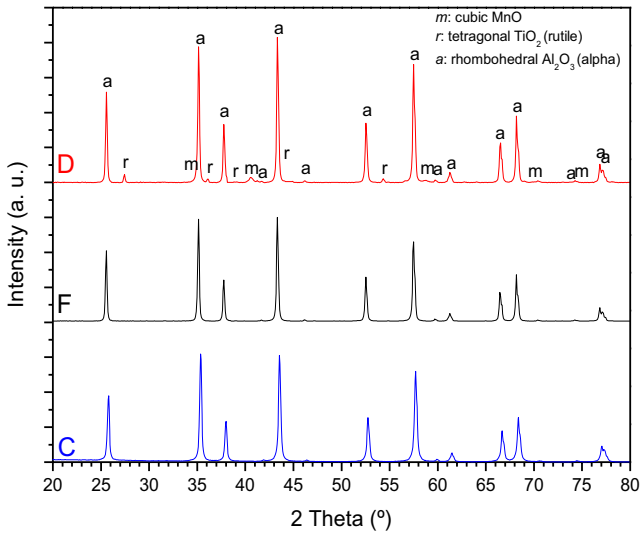

FIGURE 3 X-ray spectra of undoped (F, fine; C, coarse), and doped (D) alumina raw powders. Crystallographic identification according to PDF-2 ICDD database

Samples presented a shear-thinning behavior, as expected and required for tape casting slurries. The higher thixotropy corresponding to the hysteresis loop in the shear stress versus shear rate graph is most likely a consequence of the higher amount of organics. The organic additives at rest state increase considerably the viscosity. When the shear stress increases, the organic structure is destroyed, the entrapped liquid within is released, and the viscosity is reduced.[19] For all samples, at the same shear rate, shear stress and viscosity are higher when the rate is increasing, compared to the decreasing rate curve. At a shear rate of 100 s^{-1}, the mean values of viscosity are 1.89, 2.43, and 1.41 Pa·s for F, D, and C, respectively. Even using the same

solid content (21 vol%), D's viscosity is higher than F ones, due to its higher density. Consequently, the amount of organics additives added is to the slurry higher, because it is related to solid content. The coarse alumina, even added with 25 vol%, presented the lower values of viscosity, due to its higher average particle size compared to F and D.

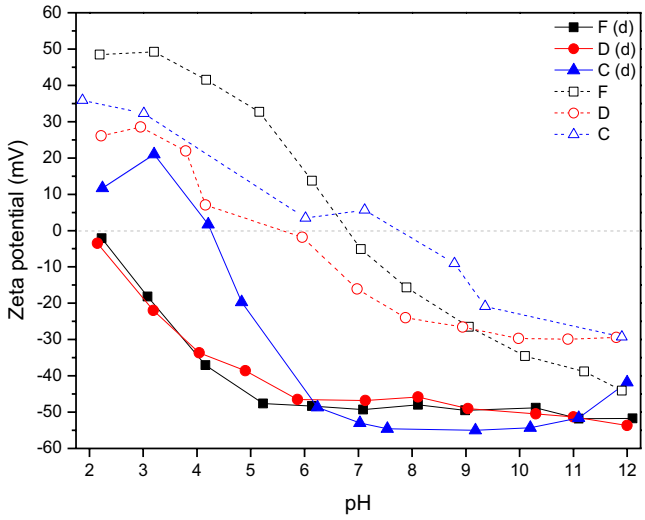

FIGURE 4 Zeta potential vs pH of oxide powders in aqueous suspensions without (dashed) and with (straight) the addition of 1 wt% dispersant referred to powder content. Suspensions containing dispersant are marked with (d) in the graphic's legend. C, coarse alumina; D, doped fine alumina; F, fine alumina

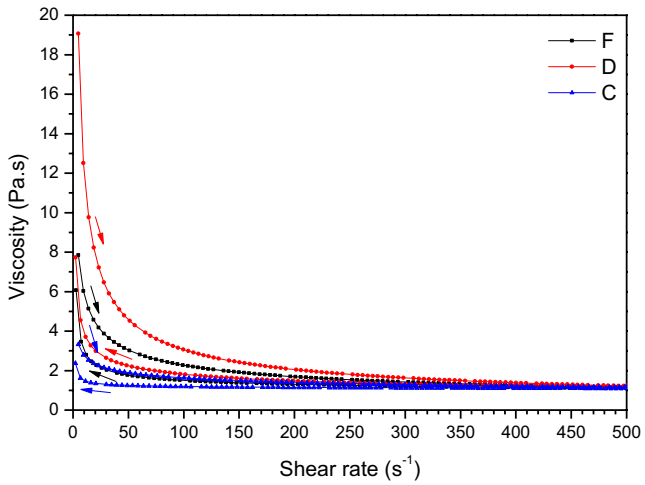

FIGURE 5 Rheological behavior of slurries used for processing tapes at varying shear rates fitted by the Herschel-Bulkley's model. Arrows indicate the direction of curves, according to shear rate variation. C, coarse alumina; D, doped fine alumina; F, fine alumina

3.3 | Characterization of tapes

Green cast tapes presented suitable flexibility and easy handling after drying, with no visible defects like cracks and bubbles (Figure 6). The thickness varied in the range of 100-145 μm. Figure 7 shows the surface micrographs of F, C, and D tapes, as analyzed by SEM. Pores can be observed at both top and bottom surfaces. However, the bottom surfaces (smooth), which were in contact with the carrier, seem to be visually less porous than their respective top surfaces (rough). This gradient is caused by the evaporation of water and its elimination through the surface in contact with air. Furthermore, the binder takes more time to consolidate by coalescence and, due to this, clusters of the binder are formed. They migrate in the same direction of the water (from the bottom to the top) during drying and form groups on the top surface.[27]

Figure 8 shows the thermal analyses (TG and DSC) of the fine alumina tapes. Mass starts to decrease at ~215°C and stays constant at ~530°C, due to the elimination of residual water and after to the burnout of volatile organics. The sample presented a final mass loss of ~15%. Exothermic peaks are observed at 268, 357, and 500°C, corresponding to the combustion of organic additives of different molecular chain lengths.

4 | CONCLUSIONS

In this work, thin ceramic samples from undoped and doped alumina powders were successfully processed and shaped by tape casting. As-received powders presented unimodal distributions, with irregular faceted shapes for alumina powders. The use of dispersant assisted the stabilization of particles and decreased the pH value at the isoelectric point. Rheological analyses for slurries showed shear-thinning and thixotropic behavior. Tapes presented different morphologies on top and bottom surfaces, with higher regularity in the

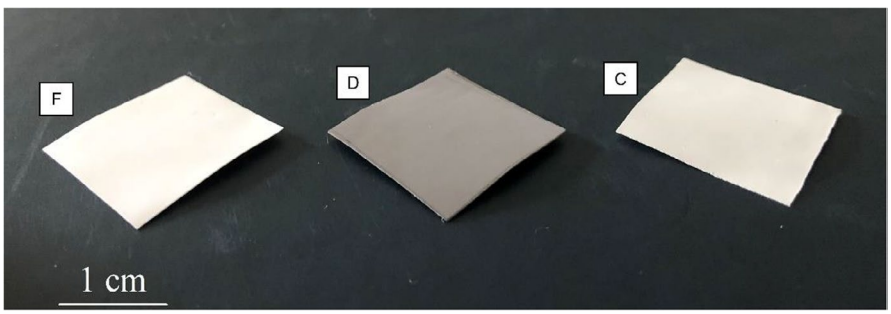

FIGURE 6 Samples of green dried tapes: C, coarse alumina; D, doped fine alumina; F, fine alumina

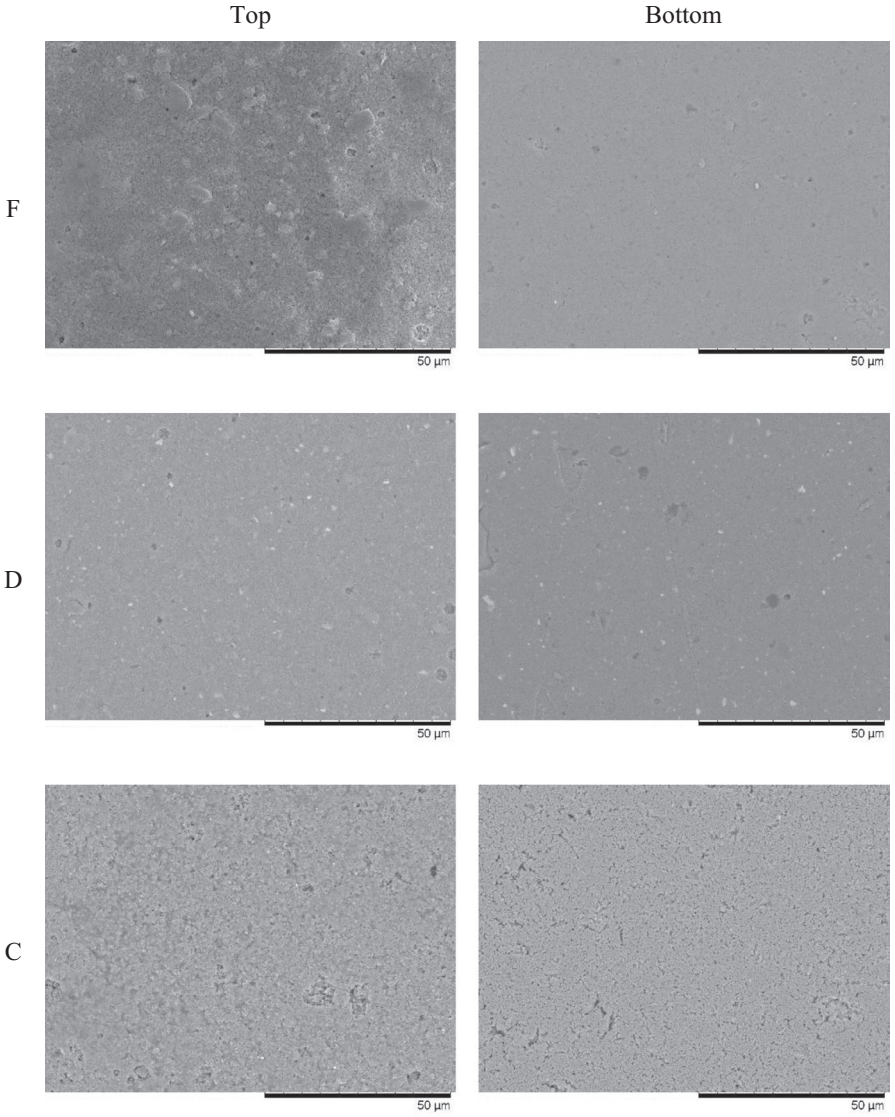

FIGURE 7 SEM micrographs of top and bottom surfaces of green dried tapes: C, coarse alumina; D, doped fine alumina; F, fine alumina

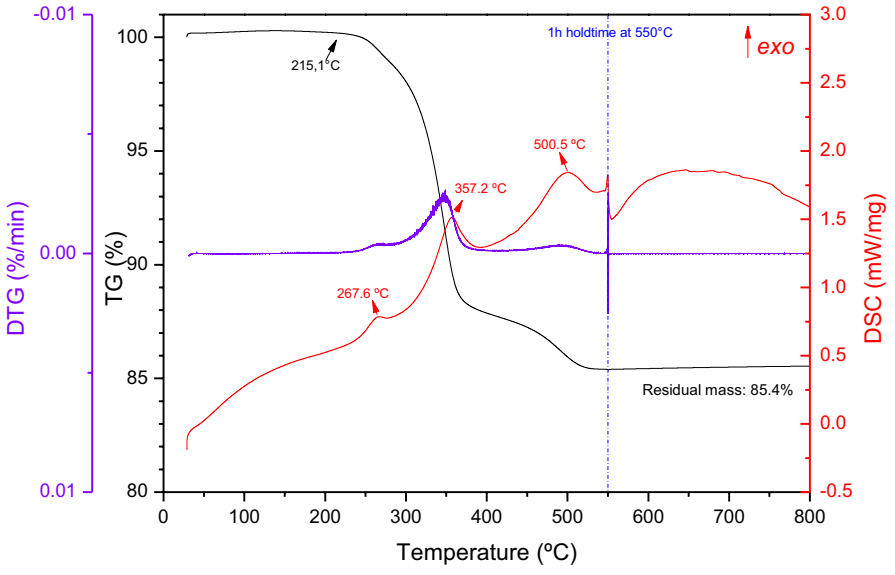

FIGURE 8 Thermal analysis (TG/DSC) of a single fine alumina tape

last ones. Thermogravimetric analyses showed a first weight loss starting at ~215°C due to the removal of residual water and small-chain organic additives. A larger weight loss and a small expansion were observed in the range of 300-525°C due to the burnout of long-chain organics.

ACKNOWLEDGMENTS

This work was supported by the International Cooperation Program Probral at the Hamburg University of Technology, which was financed by the Brazilian Federal Agency for Support and Evaluation of Graduate Education (CAPES), and the German Academic Exchange Service (DAAD). The experimental work at TUHH was partly funded by the German Research Foundation (DFG), Project 192346071, SFB 986 (C5), and by the Project CAPES/PRINT 88881.310728/2018-0.

ORCID

Marcelo Daniel Barros https://orcid.org/0000-0002-6105-5828
Dachamir Hotza https://orcid.org/0000-0002-7086-3085
Rolf Janssen https://orcid.org/0000-0001-7054-0510

REFERENCES

1. Mistler RE, Twiname ER. Tape casting: theory and practice. Westerville, OH: The American Ceramic Society; 2000.
2. Sōmiya S, editor. Handbook of advanced ceramics: materials, applications, processing, and properties. London: Academic Press; 2013.
3. Jabbari M, Bulatova R, Tok AIY, Bahl CRH, Mitsoulis E, Hattel JH. Ceramic tape casting: a review of current methods and trends with emphasis on rheological behaviour and flow analysis. Mater Sci Eng B Solid-State Mater Adv Technol. 2016;212:39–61.
4. Barry Carter C, Grant Norton M. Ceramic materials: science and engineering. New York, NY: Springer; 2007.
5. Hotza D. Artigo revisão: colagem de folhas cerâmicas. Cerâmica. 1997;43:159–66.
6. Riedel R, Chen I-W, editors. Ceramics science and technology, volume 3: synthesis and processing. Weinheim: Wiley; 2011.
7. Nishihora RK, Rachadel PL, Quadri MGN, Hotza D. Manufacturing porous ceramic materials by tape casting -A review. J Eur Ceram Soc. 2018;38(4):988–1001.
8. Hotza D, Nishihora RK, Machado RAF, Geffroy P, Chartier T, Bernard S. Tape casting of preceramic polymers toward advanced ceramics: a review. Int J Ceram Eng Sci. 2019;1(1):21–41.
9. Chartier T, Rouxel T. Tape-cast alumina-zirconia laminates: processing and mechanical properties. J Eur Ceram Soc. 1997;17(2–3):299–308.
10. Greenwood R, Roncari E, Galassi C. Preparation of concentrated aqueous alumina suspensions for tape casting. J Eur Ceram Soc. 1997;17(12):1393–401.
11. Albano MP, Genova LA, Garrido LB, Plucknett K. Processing of porous yttria-stabilized zirconia by tape-casting. Ceram Int. 2008;34(8):1983–8.
12. Moreno V, Hotza D, Greil P, Travitzky N. Dense YSZ laminates obtained by aqueous tape casting and calendering. Adv Eng Mater. 2013;15(10):1014–8.
13. Snijkers F, de Wilde A, Mullens S, Luyten J. Aqueous tape casting of yttria stabilised zirconia using natural product binder. J Eur Ceram Soc. 2004;24(6):1107–10.
14. Hotza D, Greil P. Review: aqueous tape casting of ceramic powders. Mater Sci Eng A. 1995;202(1–2):206–17.
15. Rahaman MN. Ceramic processing and sintering, 2nd edn. Boca Raton, FL: CRC Press; 2003.
16. Chartier T, Bruneau A. Aqueous tape casting of alumina substrates. J Eur Ceram Soc. 1993;12(4):243–7.
17. Gutiérrez CA, Moreno R. Influence of slip preparation and casting conditions on aqueous tape casting of Al2O3. Mater Res Bull. 2001;36(11):2059–72.
18. Pugh RJ, Bergstrom L. Surface and colloid chemistry in advanced ceramics processing, 1st edn. Boca Raton, FL: CRC Press; 1993.
19. Moreno R. Reología de suspensiones cerámicas. Madrid: Consejo Superior de Investigaciones Científicas; 2005.
20. Pagnoux C, Chartier T, Granja MF, Doreau F, Ferreira JM, Baumard JF. Aqueous suspensions for tape-casting based on acrylic binders. J Eur Ceram Soc. 1998;18(3):241–7.
21. Bitterlich B, Lutz C, Roosen A. Rheological characterization of water-based slurries for the tape casting process. Ceram Int. 2002;28(6):675–83.
22. Daniel Barros M, Jelitto H, Hotza D, Janßen R. Microstructure and mechanical behavior of TiO_2-MnO doped-alumina/alumina laminates. J Am Ceram Soc. 2021;104(2):1047–57.
23. Daniel Barros M, Hotza D, Janßen R. Dopant diffusion in the interface during sintering of TiO_2-MnO doped alumina-alumina laminates. Int J Ceram Eng Sci. 2021.
24. Daniel Barros M, Rachadel PL, Fredel MC, Janßen R, Hotza D. Mechanical behaviour of zirconia-toughened alumina laminates with or without Y-PSZ intermediate layers. J Ceram Sci Tech. 2018;9:69–78.
25. Kosmulski M. Surface charging and points of zero charge, 1st edn. Boca Raton, FL: CRC Press; 2009.
26. Singh BP, Menchavez R, Takai C, Fuji M, Takahashi M. Stability of dispersions of colloidal alumina particles in aqueous suspensions. J. Colloid Interface Sci. 2005;291:181–6.
27. Albano MP, Garrido LB, Plucknett K, Genova LA. Influence of starch content and sintering temperature on the microstructure of porous yttria-stabilized zirconia tapes. J. Mater Sci. 2009;44:2581–9.

How to cite this article: Daniel Barros M, Hotza D, Janssen R. Colloidal processing and characterization of TiO_2–MnO-doped alumina/alumina slurries and tapes. *Int J Ceramic Eng Sci*. 2021;3:173–179. https://doi.org/10.1002/ces2.10087